CHEMISTRY
A EUROPEAN JOURNAL

DOI: 10.1002/chem.200701362

Ruthenium–Olefin Complexes: Effect of Ligand Variation upon Geometry

Donde R. Anderson,[a] Daniel J. O'Leary,[b] and Robert H. Grubbs*[a]

Abstract: The development of a model system to study ruthenium–olefin complexes relevant to the mechanism of olefin metathesis has been reported recently. Upon addition of the ligand precursor 1,2-divinylbenzene to $[RuCl_2(Py)_2(H_2IMes)(=CHPh)]$ (H_2IMes = 1,3-dimesityl-4,5-dihydroimidazol-2-ylidene), two ruthenium–olefin adducts are formed. Based on ^1H NMR spectroscopy experiments and X-ray crystallographic analysis, these complexes are assigned as side-bound isomers in which the olefin and H_2IMes ligands are coordinated *cis* to each other. Herein is reported an investigation of the generality of these observations through variation of the *N*-heterocyclic carbene ligand and the ligand precursor.

Keywords: alkene ligands · ligand effects · olefin metathesis · reaction mechanisms

Introduction

Olefin metathesis has become an increasingly utilized catalytic method for the formation of new carbon–carbon bonds.[1,2] The mechanism of olefin metathesis involves olefin binding to a metal alkylidene, metallacyclobutane formation and cycloreversion to provide another metal alkylidene–olefin complex. Subsequent olefin dissociation generates a metal alkylidene that can re-enter the catalytic cycle.

Mechanistic studies of ruthenium olefin metathesis catalysts **1** and **2** have revealed important details about catalyst initiation,[3–5] but until recently, little information was available about the geometry of short-lived intermediates such as the ruthenium–olefin complex[6,7] and ruthenacyclobutane complex.[8–11]

Of particular interest for the further development of enantioselective and *E*/*Z*-diastereoselective catalysts is the geometry of ruthenium–olefin complexes. Coordinatively unsaturated complex **3** can bind an olefin to form either complex **4a**, in which the olefin is *trans* to the L-type ligand, or **4b** in which the olefin is *cis* to the L-type ligand (Scheme 1). Both geometries are supported by previously studied ruthenium–olefin complexes **5**[6] and **6a**,**b**.[7]

We recently reported the synthesis and characterization of ruthenium–olefin complexes formed utilizing 1,2-divinylbenzene as a ligand precursor.[7] Complexes **6a**,**b** in which the ruthenium center is coordinated to a pendant olefin were isolated as a mixture of isomers and fully characterized by 1D and 2D NMR spectroscopy. Both isomers are side-bound and undergo interconversion at ambient temperatures. A parallel computational study, reported in the same paper, found the side-bound isomers were preferred when the calculations included a solvent continuum model. Herein, we present the synthesis and characterization of a series of analogous ruthenium–olefin complexes in which the NHC ligand or chelating olefin ligand is varied.

Results and Discussion

Fluorinated NHC complex: Recently, the increased initiation efficiency of complex **7** was reported and postulated to result from fluorine-assisted phosphine dissociation (Scheme 2).[12] Although no solid-state Ru–F interaction is observed for complex **7**, possibly due to the steric bulk of the PCy_3 ligand, a Ru–F interaction (3.2 Å) is observed for chelating ether complex **8** in the solid state. Complex **10** was targeted to explore the effect of decreasing NHC steric bulk relative to H_2IMes and to determine if a Ru–F interaction could be observed in solid-state or solution-phase studies.

[a] D. R. Anderson, Prof. R. H. Grubbs
Arnold and Mabel Beckman Laboratories of Chemical Synthesis
Division of Chemistry and Chemical Engineering
California Institute of Technology, Pasadena, CA 91125 (USA)
Fax: (+1) 626-564-9297
E-mail: rhg@caltech.edu

[b] Prof. D. J. O'Leary
Department of Chemistry, Pomona College
645 N. College Ave., Claremont, CA 91711 (USA)

Supporting information for this article is available on the WWW under http://www.chemeurj.org/ or from the author.

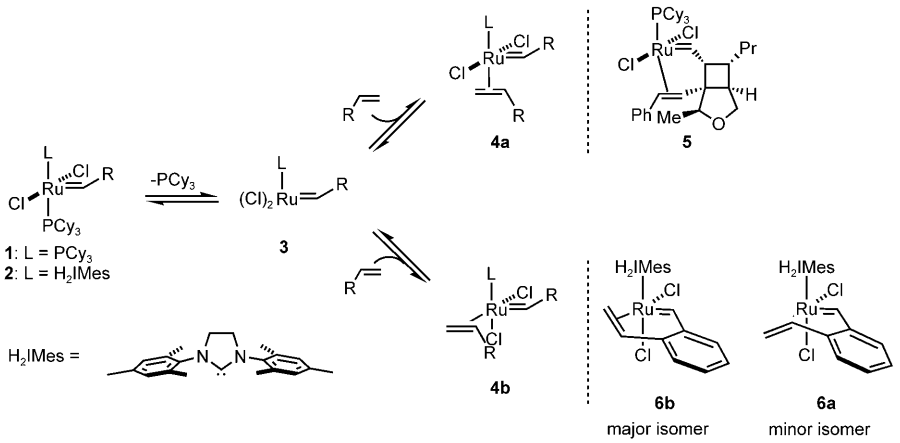

Scheme 1. Initiation and olefin-binding steps of the olefin metathesis catalytic cycle.

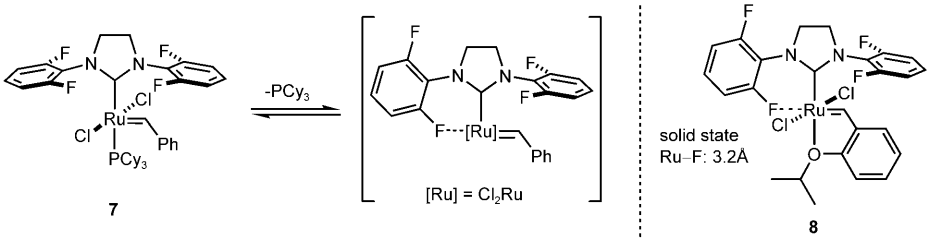

Scheme 2. Ruthenium complexes of a fluorine-containing NHC.

Upon addition of 1,2-divinylbenzene (**9**) to complex **7** in C_6D_6, three new species with benzylidene resonances (H_α) at δ 17.44, 16.86, and 16.61 ppm are initially observed by ^{1}H NMR spectroscopy [Eq. (1)]. After 4 h at 22 °C, the resonance at 17.44 ppm is no longer observed and we attribute this resonance to an unidentified intermediate associated with complex formation. Upon precipitation with pentane, a yellow solid comprised of the two ruthenium–olefin complexes (isomers of **10**) with resonances at 16.57 and 16.42 ppm (1:1) in CD_2Cl_2 were isolated. Our previous work with complexes **6a**/**6b** demonstrated that the chemical shifts and percent composition of different complexes could be solvent- and temperature-dependent, hence the discrepancy between the benzylidene chemical shifts in different solvents. Unlike **6a**/**6b**, no exchange between the two **10a**/**10b** isomers was observed in 2D-EXSY experiments performed in CD_2Cl_2 at room temperature.

1D ^{1}H{^{19}F} heteronuclear Overhauser (HOESY) experiments were performed to identify these isomers by examining possible through-space interactions between olefinic protons and the fluorine atoms on the NHC ligand (Figures 1 and 2). The species with a benzylidene resonance at 16.57 ppm is assigned as isomer **10a** based on an HOE interaction between H_a and a ^{19}F resonance at −117.9 ppm. The second species at 16.42 ppm is assigned as isomer **10b** due to an observed HOE interaction between H_c and a fluorine resonance at −118.2 ppm. We note that the vicinal olefinic protons H_b and H_c of **10a** and **10b**, similar to complexes **6a** and **6b**, are significantly shifted upfield to 3–4 ppm (Figure 2). HOE interactions are also observed between fluorine resonances at −113.7 ppm and −115.7 ppm and benzylidene protons (H_α) of **10a** and **10b**, respectively. Finally, HOE interactions are observed between all ^{19}F/H_{ortho} spin pairs.

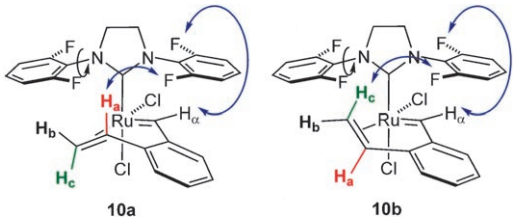

Figure 1. Structural assignment of solution isomers of **10** based on observed HOEs (arrows). Unhindered N–C bond rotation shown with black arrows.

The ^{19}F NMR spectrum of complexes **10a** and **10b** in 1:1 CD_2Cl_2/[D_2]TCE at room temperature displays four sharp peaks and one broad signal, rather than the eight signals expected if the system is in slow exchange (Figure 3). We hypothesized that exchange at room temperature may broaden the four unobserved signals in the ^{19}F NMR spectrum; eight fluorine resonances were observed when the sample was cooled to −85 °C. Together with the 1D HOESY data, these results are consistent with hindered rotation of the aryl ring near the quadrant containing the benzylidene moiety and free rotation of the aryl ring above the open quadrant at room temperature (Figure 1). For comparison, N–C bond rotation is not observed for complexes H_2IMes-substituted ana-

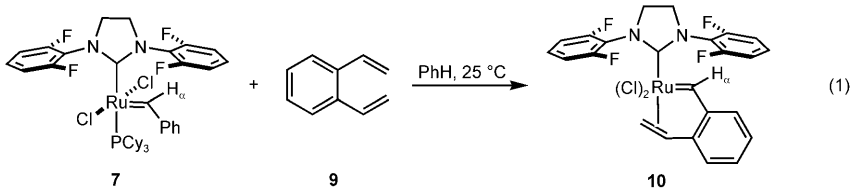

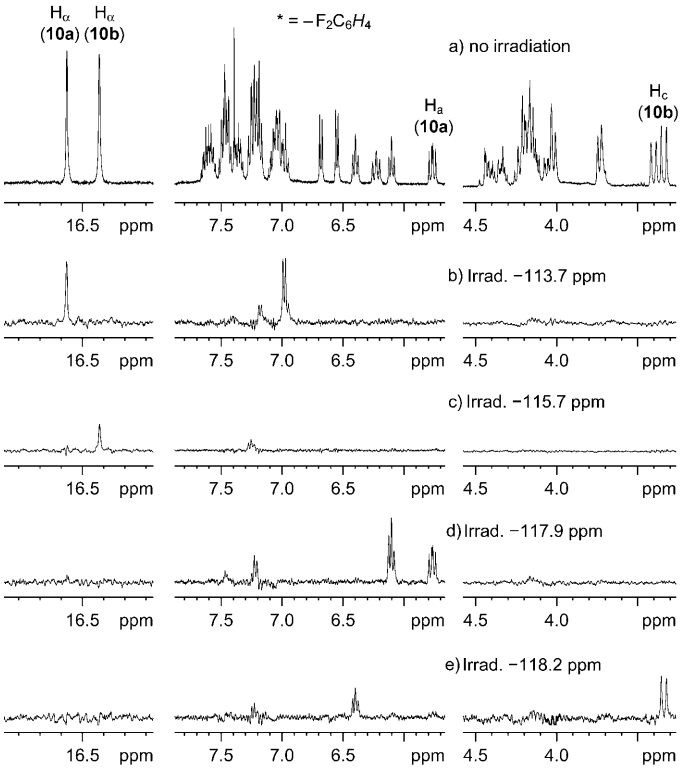

Figure 2. Benzylidene (H_α) and olefin proton-containing portions of 1D ^1H–^{19}F HOESY spectra of **10a** and **10b** in CD_2Cl_2 after irradiation at a) no irradiation, b) −113.7 ppm, c) −115.7 ppm, d) −117.9 ppm, e) −118.2 pm.

logs **6a** and **6b**, although Ru−C_{NHC} bond rotation is observed.[7]

In the ^1H NMR spectrum of complexes **10a** and **10b**, the benzylidene protons are observed to be quartets when the spectral data is subjected to Gaussian resolution enhancement (Figure 4). ^1H–^1H coupling is observed between H_α and H_b and between H_α and its *ortho*-disposed aromatic proton for both isomers ($J = 1$ Hz). Additionally, $^1H\{^{19}F\}$ decoupling experiments demonstrated that each benzylidene resonance is also coupled with a single fluorine resonance. We believe that this coupling is a result of a through space, rather than through-bond interactions. Indeed, H_a and any of the fluorine nuclei are separated by seven sigma bonds and the couplings involve specific pairs of nuclei. If the couplings occurred through the bonding framework, then one might have expected to see coupling between each H_a and two fluorine nuclei. These results are also consistent with the observed HOE interactions between fluorine resonances at δ −113.7 ppm and −115.7 ppm and benzylidene protons (H_α) of **10a** and **10b**, respectively.

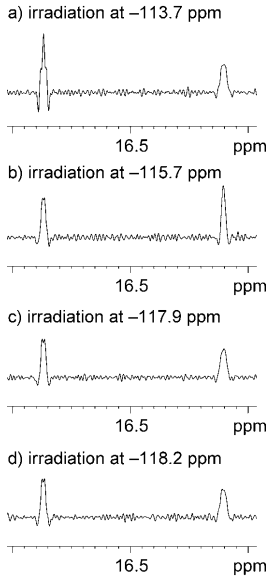

Figure 4. Benzylidene (H_α) region of $^1H\{^{19}F\}$ NMR spectra (Gaussian resolution enhanced) acquired with continuous-wave ^{19}F irradiation at frequencies a) −113.7 ppm, b) −115.7 ppm, c) −117.9 ppm, d) −118.2 ppm to elucidate ^1H–^{19}F spin–spin coupling pathways in complexes **10a** and **10b**.

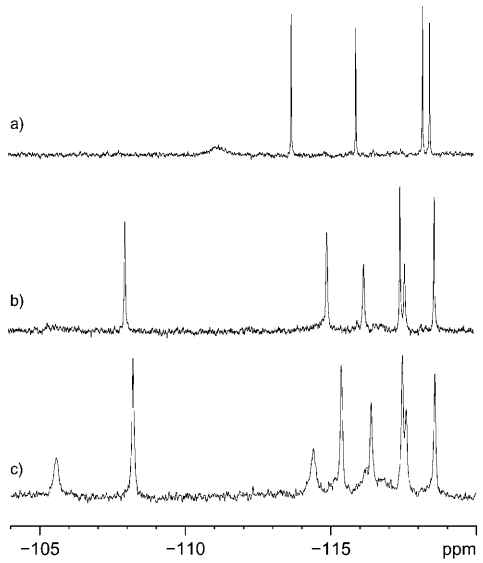

Figure 3. Variable-temperature ^{19}F NMR spectra for a solution of isomers **10a** and **10b** in 1:1 CD_2Cl_2/[D_2]TCE taken at a) 22 °C, b) −60 °C, c) −80 °C.

X-ray quality crystals grown from a solution of **10a** and **10b** provided a solid-state structure of side-bound isomer **10b** (Figure 5). The ruthenium center has a distorted square-pyramidal geometry. Unlike complex **7**, the NHC plane of complex **10a** is not significantly distorted from the ruthenium benzylidene plane. Although complex **10a** contains a side-bound olefin, the terminal methylene group of the olefin is directed toward the region of the NHC, unlike the solid-state structure obtained for complex **6b**. Interestingly, no evidence for a Ru–F interaction (shortest Ru···F 3.82 Å) is observed despite a relatively open steric environment near the quadrant of the fluorinated aryl ring. The C−C bond length of the coordinated olefin is 1.383(3) Å, which is ca. 0.05 Å shorter than that of free styrene and complex

6b. All other bond lengths and angles are similar to those observed for complex **6b**.[7]

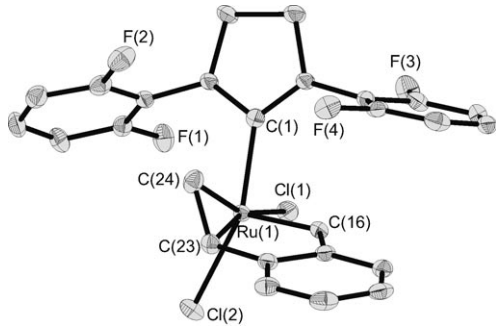

Figure 5. Solid-state drawing of **10b**. Thermal ellipsoids drawn at 50% and hydrogens omitted for clarity. Selected bond lengths [Å] and angles [°]: Ru–C(1) 2.0397(19), Ru–C(26) 1.840(2), Ru–Cl(1) 2.3865(5), Ru–Cl(2) 2.3768(5), Ru–C(23) 2.2283(19), Ru–C(24) 2.203(2), C(23)–C(24) 1.383(3), Cl(1)-Ru-Cl(2) 87.941(18), C(1)-Ru-Cl(2) 153.28(5), C(23)-Ru-Cl(1) 162.84(5), C(24)-Ru-Cl(1) 160.75(6).

Bulkier NHC complex: To explore the effect of increasing the steric bulk of the NHC on olefin binding geometry, H_2DIPP-containing (H_2DIPP = 1,3-di(2,6-diisopropylphenyl)-4,5-dihydroimidazol-2-ylidene) complexes were prepared. Upon addition of 1,2-divinylbenzene (**9**) to a solution of complex **11**[13] in benzene, two ruthenium–olefin complexes with benzylidene resonances (H_α) at δ 16.27 ppm and 16.58 ppm were isolated in a 97:3 ratio [Eq. (2)].

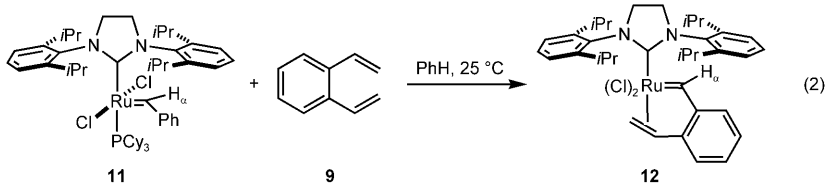

For the major isomer, 2D-NOESY experiments demonstrated Overhauser effects between olefinic proton H_b and one Me group at δ 1.46 ppm (CD_2Cl_2), and between H_c and two Me groups at 0.11 and 1.32 ppm (C_6D_6) and between H_c and an isopropyl methine proton at 2.35 ppm (C_6D_6) (Figures 6 and 7. In this case, we changed NMR solvents in order to alleviate peak overlap issues. No crosspeaks were observed between H_a and the isopropyl groups. Interestingly, an NOE interaction is also observed between the methine protons of proximal isopropyl groups spanning the olefin binding site. These interactions are consistent with isomer **12a** in which the olefin is directed toward the NHC. Due to the low concentration of the minor isomer, no structural assignment could be made. 2D-EXSY experiments did not show any exchange of the benzylidene protons of the major (**12a**) and minor isomers in CD_2Cl_2 at 22 °C.

Several characteristic NMR shifts and couplings are observed for complex **12a**. The vicinal protons H_b and H_c are significantly shifted upfield to 3–4 ppm. Long-range COSY experiments indicate ^{1}H–^{1}H coupling between the benzylidene proton (H_α) and H_b of the coordinated olefin.

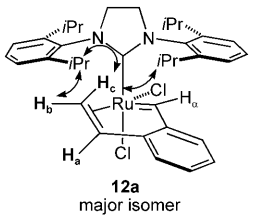

Figure 6. Structural assignment of major solution isomer of **12** based on observed NOEs (arrows).

Interestingly, upon addition of **9** to complex **11**, a benzylidene resonance at δ 16.49 ppm is initially observed in the ^{1}H NMR spectrum of the crude reaction, but disappears after a few hours at room temperature. Unlike other observed intermediates, a relatively high conversion (25%) of this unstable intermediate was initially observed. However, attempts to isolate or further characterize this intermediate by VT NMR spectroscopy were unsuccessful.

Although suitable crystals of complex **12** could not be isolated, ruthenium-containing decomposition products were characterized by X-ray crystallography. The solid-state structure obtained from these crystals show three components (Figure 8): free H_2DIPP, O=PCy$_3$ and hexacoordinate ruthenium center **13** (Figure 9 and Supporting Information). The benzylidene moiety has been oxidized to a benzoate group which acts as a chelating ligand for the Ru^{IV} complex. The source of the oxygen atoms may be either O_2 or H_2O.

Chiral NHC complex: Chiral complex **14** was also investigated as a ruthenium precursor. Upon addition of **9** to **14** in pentane, three isomers with benzylidene resonances (H_α) at 16.25, 15.57 and 15.37 ppm are isolated in a 3:6:1 ratio

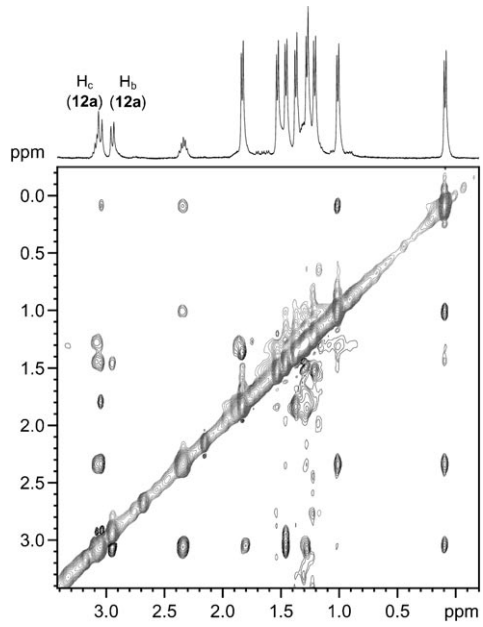

Figure 7. Olefin and alkyl-group region of a 2D-NOESY spectrum of **12** in CD_2Cl_2.

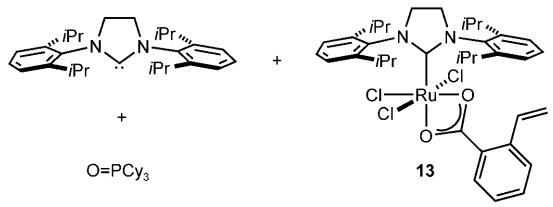

Figure 8. Decomposition products of complex **12**.

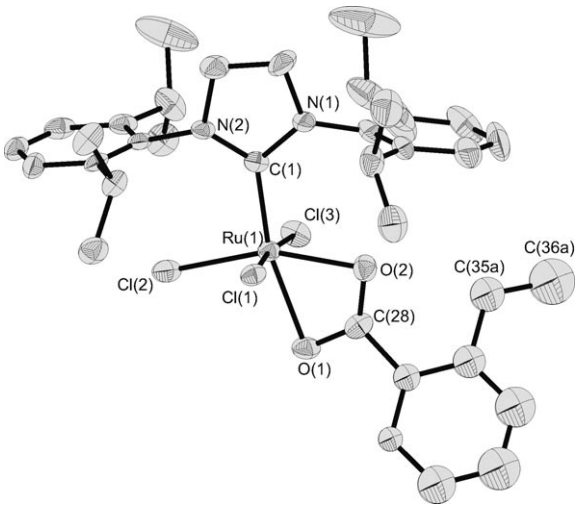

Figure 9. Solid-state drawing of **13**. Thermal ellipsoids drawn at 50% and hydrogens omitted for clarity. Selected bond lengths [Å] and angles [°]: Ru–C(1) 1.978(3), Ru–O(1) 2.229(2), Ru–O(2) 2.114(2), Ru–Cl(1) 2.3529(8), Ru–Cl(2) 2.3125(9), Ru–Cl(3) 2.3247(9), Cl(1)-Ru-Cl(3) 173.16(3), C(1)-Ru-O(1) 165.36(10), Cl(2)-Ru-O(2) 158.62(6).

[Eq. (3)]. Unlike previously investigated complexes, four side-bound ruthenium–olefin complexes (**15a–d**, Figure 10) are possible due to the mono-*ortho* substituted aryl groups on the NHC.

Overhauser effects were observed between H_b of both major isomers and Me groups on the NHC in 2D-NOESY experiments (Figures 10 and 11). These isomers are assigned as **15a** and **15b** because it would not be expected that H_b of either **15c** or **15d** would be in close proximity to an isopropyl group. No NOEs are observed for H_c of either isomer with the isopropyl groups. The isomer in largest abundance ($H_\alpha = 15.57$ ppm) is assigned as isomer **15a** due to an observed NOE between H_c and an *ortho*-aryl proton the NHC. The other major isomer ($H_\alpha = 16.25$ ppm) is assigned as isomer **15b** based on an observed NOE between H_a and a

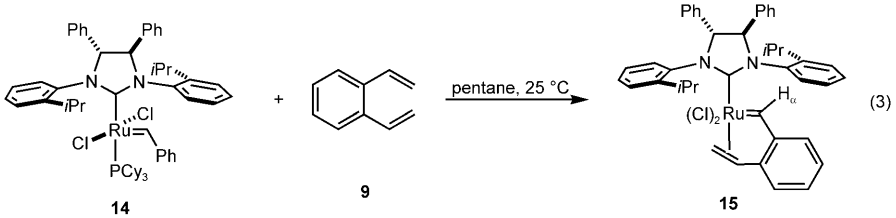

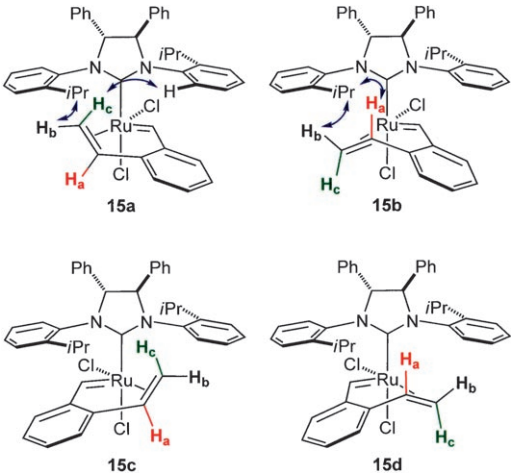

Figure 10. Possible side-bound geometries for complex **15**. Observed NOEs shown with arrows.

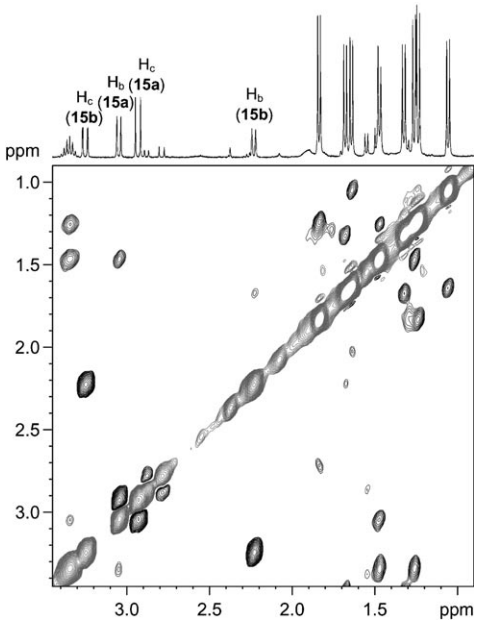

Figure 11. Olefin and alkyl-group region of a 2D-NOESY spectrum of **15** in CD_2Cl_2.

Me group of an isopropyl moiety. No assignment could be made for the isomer in smallest concentration ($H_\alpha =$ 15.37 ppm) due to the absence of any diagnostic NOE cross-peaks.

2D-EXSY experiments performed in CD_2Cl_2 at 19 and 40 °C did not reveal any exchange processes in this complex. Several characteristic NMR shifts and couplings are observed for the three isomers of **15**. The olefinic protons for all 3 observed isomers are shift-

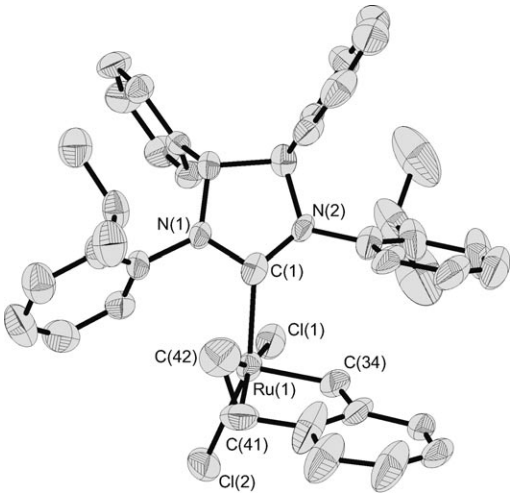

Figure 12. Solid-state drawing of **15a**. Thermal ellipsoids drawn at 50% and hydrogens omitted for clarity. Selected bond lengths [Å] and angles [°]: Ru–C(1) 2.045(5), Ru–C(26) 1.849(5), Ru–C(41) 2.227(6), Ru–C(42) 2.184(6), Ru–Cl(1) 2.4027(12), Ru–Cl(2) 2.3881(12), C(41)–C(42) 1.318(7), Cl(1)-Ru-Cl(2) 86.81(5), C(1)-Ru-Cl(2) 154.55(14), C(41)-Ru-Cl(1) 163.82(15).

ed upfield to 2–3.5 ppm. The benzylidene resonance (H_α) of **15a** exhibits a long-range coupling to H_b at 3.05 ppm; similarly, H_α of **15b** exhibits a long-range coupling to H_b at 2.23 ppm.

X-ray quality crystals grown from slow diffusion of pentane into a concentrated solution of **15** in THF provided a structure of side-bound olefin complex **15a** (Figure 12). The bond lengths and angles are similar to those observed for other ruthenium–olefin complexes.

Phosphine complex: To examine the possibility that phosphine and NHC complexes could have different preferred olefin-binding geometries, a phosphine analogue to complexes **10**, **12** and **15** was prepared. Bisphosphine complex **1**, in the presence of 1 equiv divinylbenzene (**9**) showed low reactivity as monitored by ^{1}H NMR spectroscopy. However, utilizing bispyridine complex **16** as a ruthenium precursor in presence of **9**, two new ruthenium-olefin complexes (**17**) with benzylidene resonances (H_α) at 17.85 and 17.62 ppm were isolated in a 9:1 ratio [Eq. (4)].

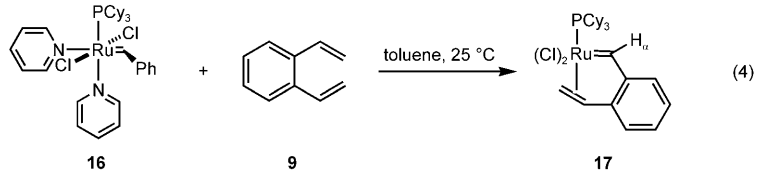

2D-NOESY experiments demonstrated cross peaks between olefinic proton H_b of the major isomer and cyclohexyl protons (Supporting Information). No NOE crosspeaks are observed in the major isomer between H_a and the alkyl region. Olefinic proton H_c overlaps with a cyclohexyl resonance, thus making it difficult to determine if there are NOEs between H_c and the cyclohexyl protons. Although the evidence is based upon a single NOE observation, we hypothesize that the major isomer is side-bound isomer **17b** (figure 13). Because of its low concentration, no cross peaks were observed for the minor isomer.

2D-EXSY experiments conducted in CD_2Cl_2 at room temperature demonstrated exchange between all olefinic protons of the major and minor isomers. The benzylidene resonances also undergo exchange with each other. This suggests that phosphine complex **17** exhibits behaviour similar to that of the parent NHC olefin complex **6** from the standpoint of Ru–olefin binding lability.

We were unable to grow crystals of **17** suitable for X-ray crystallography. Unfortunately, the ruthenium olefin complex isomers of **17** decompose at room temperature in hours.

Bulkier olefin complex: To examine the steric effect of binding a 1,1-disubstituted olefin, diene **19** was synthesized [Eq. (5)]. Upon addition of **19** to a solution of bispyridine complex **18**, several new ruthenium-olefin complexes are formed. In CD_2Cl_2, the two major benzylidene resonances are at δ 15.86 and 15.50 ppm (4:1).

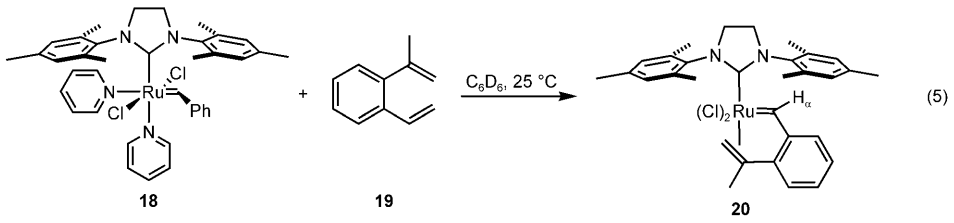

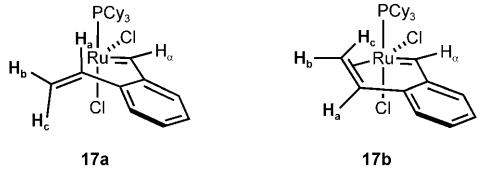

Figure 13. Possible side-bound geometries for complex **17**. An NOE for the major isomer is observed between H_b and cyclohexyl protons.

2D-NOESY experiments demonstrate NOEs between olefinic proton H_c of the major isomer (assigned on the basis of HSQC and COSY-LR experiments) and Me groups of H_2IMes at 1.44 and 2.73 ppm (which are in exchange as indi-

cated by 2D-EXSY experiments) (Figures 14 and 15). These interactions are consistent with solution-phase structure **20a** in which the terminal methylene group of the olefin is directed toward the NHC.

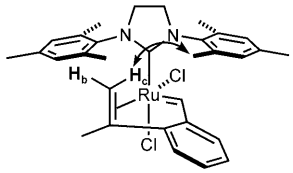

20a
major isomer

Figure 14. Structural assignment of major solution isomer of **20** based on an observed NOE (arrow). Ru–C_{NHC} bond rotation shown with the arrow.

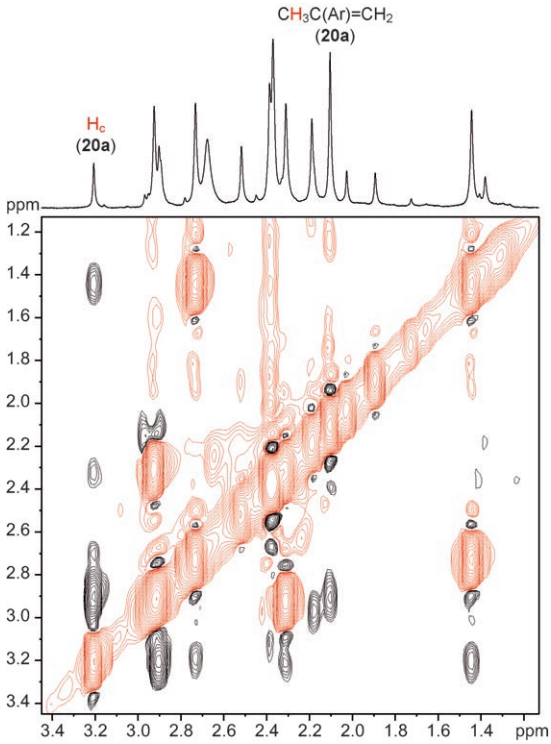

Figure 15. 2D-NOESY/EXSY spectrum of **20**.

2D-EXSY experiments demonstrate exchange of aryl, NHC backbone, and Me protons of **20a**, but not of benzylidene or olefinic protons. This data is consistent with chemical shift timescale Ru–NHC rotation rather than interconversion of the two isomers. COSYLR experiments indicate interactions between H_α and an adjacent aryl proton of **20a**. Additionally, a long-range interaction is observed between H_α and an olefinic proton H_b at 2.94 ppm. NOEs are also observed between H_α and two Me groups (2.92 and 2.35 ppm) that are in mutual exchange.

X-ray analysis of crystals grown from a solution of **20** shows a single molecular geometry, **20a**, in which H_2IMes and the chelated ligand are bound *cis* to one another (Figure 16). Bond lengths and angles are similar to other ruthenium–olefin complexes.

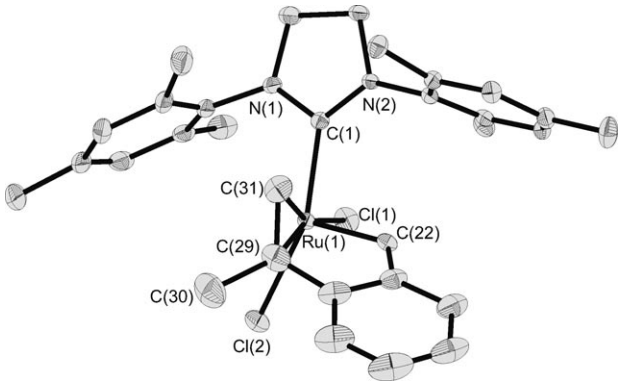

Figure 16. Solid-state drawing of **20a**. Thermal ellipsoids drawn at 50% and hydrogens omitted for clarity. Selected bond lengths [Å] and angles [°]: Ru–C(1) 2.063(2), Ru–C(26) 1.825(2), Ru–Cl(1) 2.4005(6), Ru–Cl(2) 2.3781(6), Ru–C(29) 2.249(2), Ru–C(31) 2.167(3), C(29)–C(31) 1.402(4), C(1)-Ru-Cl(2) 153.37(6), Cl(1)-Ru-Cl(2) 83.75(2), C(29)-Ru-Cl(1) 160.33(8).

Summary

Compiled in Scheme 3 is the conformational behavior of the Ru–olefin complexes studied to date.[7,11] In the work reported here, we chose to vary the NHC ligand and ligand precursor. Although not all observed solution-phase isomers could be structurally characterized, the assignable isomers of complexes **10**, **12**, **15**, **17** and **20** were determined to be side-bound isomers in which the NHC (or PCy_3) are coordinated *cis* to the chelated olefin. The dynamics of the NHC ligand appear to vary within the complexes studied thus far. Notably, the fluorinated NHC ligand appears to have differential mobility in which the aryl group lying over the benzylidene is static on the NMR chemical shift timescale, whereas the other aryl group is dynamic. Ru–NHC rotation has been observed in divinylbenzene adducts (**6b**, **20a**) with the H_2IMes ligand; interestingly this rotation is only observed in complexes in which the terminal methylene is pointing towards the ligand.

In characterizing the side-bound ruthenium–olefin complexes, the bound olefin can either be directed up towards or away from the NHC/PCy_3 ligand. In solution, the former orientation appears to be favored in all side-bound complexes with the exception of the fluorinated NHC complex **10**, where both side-bound conformations are equally populated. The olefin dynamics in most of these systems appears to be slow on the NMR chemical shift timescale: facile intramolecular exchange is only observed in the parent NHC complex **6** and PCy_3 analogue **17**.

Although we cannot rule out alternate unstable geometries that might be formed under kinetic conditions, complexes prepared from 1,2-divinylbenzene derivatives appear to have a preference for side bound complexes. Complexes

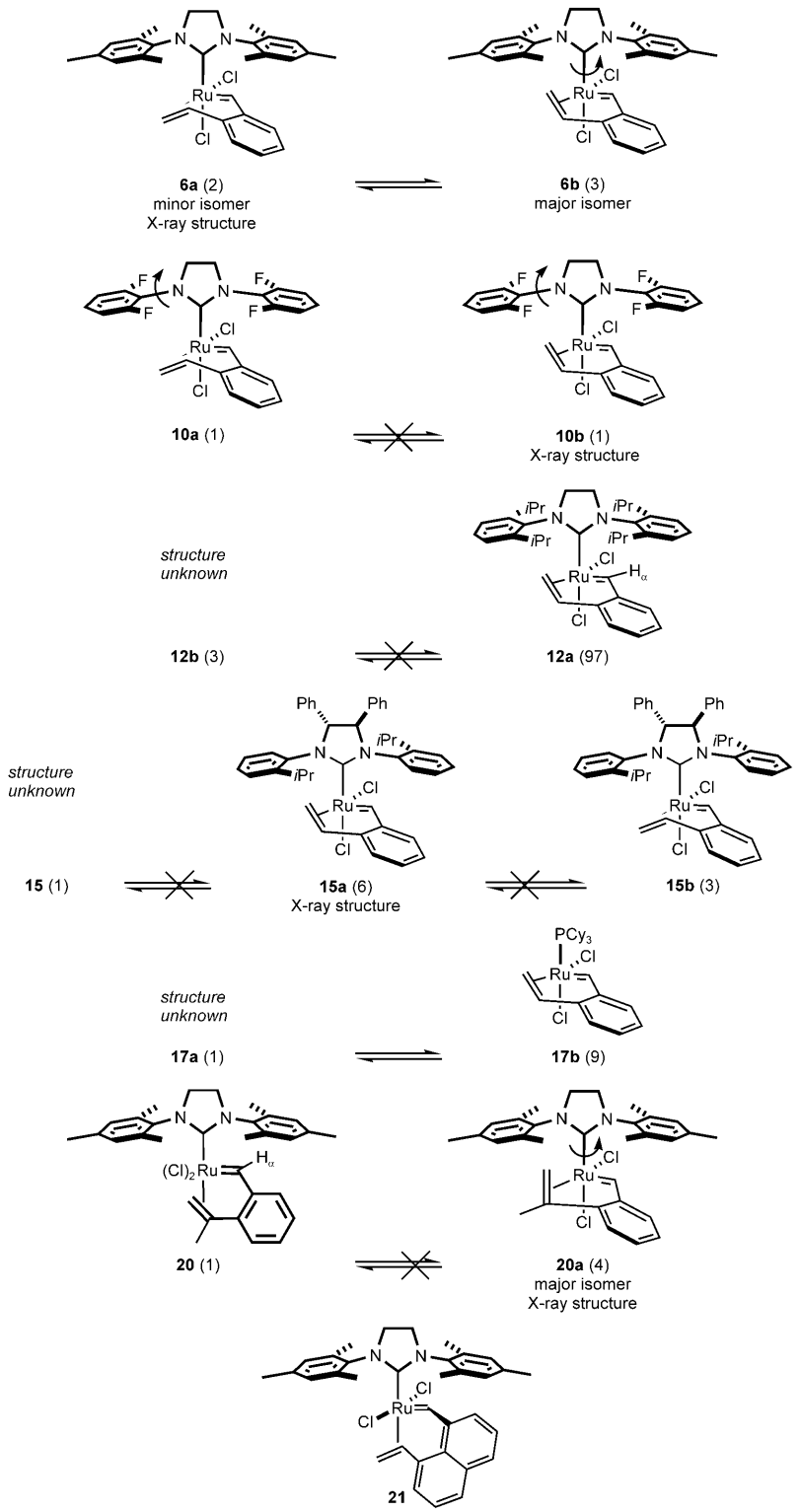

Scheme 3. Comparison of the solution-state conformational behavior of complexes **6**,[7] **10**, **12**, **15**, **17**, **20** and **21**.[11] The relative amount of each isomer is indicated in the parentheses next to the compound identifier. Curved arrows indicate bond rotations occurring on the NMR chemical shift timescale; equilibrium arrows indicate room-temperature interconversion of olefin complexes. If the solid-state structure of a complex is known, then it is denoted with the descriptor "X-ray structure."

that have been demonstrated to prefer bottom-bound olefin geometries include Snapper's 1,2-divinylcyclobutane derivative **5** and Piers and co-workers' recently reported 1,3-divinylnaphthalene complex **21**. In the latter system, which was unstable above −20 °C, the bottom bound geometry was inferred from the absence of any NOE interactions between the olefin resonances and those arising from the H_2IMes ligand. Given that these NOE interactions are quite large and readily observed in side bound complexes (e.g., **6**), this inference is justified.

Additionally, Piers and coworkers suggest that downfield benzylidene ^{1}H and ^{13}C resonances (18.13 ppm/317.3 ppm), relative to those in complexes **6a/b** (16.34 ppm/300.3 ppm and 16.17 ppm/296.9 ppm) as additional evidence of a bottom versus side-bound geometry.

The work reported here suggests that NHC-derived Ru–olefin complexes derived from 1,2-divinylbenzene are stable species and tend to adopt side-bound geometries but variable ligand dynamics. Additionally, new NMR spectroscopy metrics (long-range H_α–olefin couplings, ^{1}H–^{19}F couplings) for characterizing these complexes have been observed and may prove useful in future studies of related systems.

Acknowledgement

The authors thank Materia Inc., Jacob M. Berlin and Tobias Ritter for generous donation of ruthenium complexes. Lawrence M. Henling and Dr. Michael Day are acknowledged for X-ray crystallographic analysis. D.R.A. acknowledges NSF and NDSEG predoctoral fellowships. D.J.O. thanks the Mellon Foundation for support. R.H.G. was supported by the NSF (CHE-0410425).

[1] R. H. Grubbs, Handbook of Metathesis, Wiley-VCH, Weinheim, **2003**.
[2] K. J. Ivin, J. C. Mol, Olefin Metathesis and Metathesis Polymerization, Academic Press, San Diego, CA, **1997**.
[3] M. S. Sanford, J. A. Love, R. H. Grubbs, *J. Am. Chem. Soc.* **2001**, *123*, 6543–6554.
[4] M. S. Sanford, M. Ulman, R. H. Grubbs, *J. Am. Chem. Soc.* **2001**, *123*, 749–750.
[5] M. Ulman, R. H. Grubbs, *Organometallics* **1998**, *17*, 2484–2489.
[6] J. A. Tallarico, P. J. Bonitatebus, M. L. Snapper, *J. Am. Chem. Soc.* **1997**, *119*, 7157–7158.
[7] D. R. Anderson, D. D. Hickstein, D. J. O'Leary, R. H. Grubbs, *J. Am. Chem. Soc.* **2006**, *128*, 8386–8387.
[8] P. E. Romero, W. E. Piers, *J. Am. Chem. Soc.* **2005**, *127*, 5032–5033.
[9] P. E. Romero, W. E. Piers, *J. Am. Chem. Soc.* **2007**, *129*, 1698–1704.
[10] A. G. Wenzel, R. H. Grubbs, *J. Am. Chem. Soc.* **2006**, *128*, 16048–16049.
[11] E. F. van der Eide, P. E. Romero, W. E. Piers, *J. Am. Chem. Soc.* **2008**, *130*, 4485–4491.
[12] T. Ritter, M. W. Day, R. H. Grubbs, *J. Am. Chem. Soc.* **2006**, *128*, 11768–11769.
[13] M. B. Dinger, J. C. Mol, *Adv. Synth. Catal.* **2002**, *344*, 671–677.

Received: August 30, 2007
Revised: May 11, 2008
Published online: May 16, 2008

